IJAAMM

International Journal of Advances in Applied Mathematics and Mechanics

A study of two-phase Jeffery Hamel flow in a geothermal pipe

Research Article

Viona Ojiambo[a], *, Mathew Kinyanjui[b], Mark Kimathi[c]

[a] *Department of Pure and Applied Mathematics, Jomo Kenyatta University of Agriculture and Technology, Juja, 62000-00200, Nairobi, Kenya*

[b] *Department of Pure and Applied Mathematics, Jomo Kenyatta University of Agriculture and Technology, Juja, 62000-00200, Nairobi, Kenya*

[c] *Department of Mathematics, Statistics and Actuarial Science, Machakos University, Machakos, 136-90100, Machakos, Kenya*

Abstract: In this paper a two-phase convergent Jeffrey-Hamel flow in a geothermal pipe concentrated with silica particles and thermophoresis has been studied. The governing equations are equation of mass, momentum, heat transfer and concentration. These equations are transformed into nonlinear ordinary differential equations by introducing a similarity transformation. The resulting equations are then solved using the bvp4c collocation method. Results for velocity, temperature and concentration are presented for various parametric conditions. It is established that the unsteadiness parameter significantly influences the velocity, temperature and concentration in both the gaseous and the liquid phase, secondly the Reynolds'number effect in the gaseous phase velocity is more significant incomparison to the liquid phase, thirdly the variation in heat transfer as a result of the Prandtl number is more significant in comparison to the liquid phase, fourthly there is a significant effect of the control factor introduced in the concentration equation to counter silica polymerization . In conclusion, the gaseous and the liquid phase have to be accounted separately. Further, the control mechanisms used for preventing silica deposition need to be factored in the concentration equations with their ranking specification so as to monitor the growth of silica deposits.

MSC: 76Dxx • 76Txx

Keywords: Two-phase flow • Non-linear viscosity • Thermophoresis

1. Introduction

Mathematical modeling of geothermal pipes provides engineers with information on the construction and maintenance of the geothermal pipes. Research done by Polii and Abdurrachim [1] established that a geothermal pipe is a cylindrical pipe with radial direction of flow.

Two phase flow may occur in the geothermal pipe due to variation of density. Hasan and Kabir [2] studied a two-phase fluid and heat flow in a geothermal well using the drift flux approach. The well-bore was treated as heat sink of finite radius in an infinite acting medium. Resistance to heat transfer by various elements were then analyzed. A comparison study was done involving the new model and those that are often used in geothermal wells. Statistical analysis suggested that all models behaved similar, however the new mode was accurate.

There are different flow regimes that may occur in a two-phase flow. These are annular, stratified, plug, wavy amongst others. Palsson et al. [3] examined the probability of occurence of these flow regimes and he established that the pressure levels and the flow behavious are paramount in this study. The stratified wavy flow was found to be the

---

* Corresponding author.

E-mail address(es): vojiambo@jkuat.ac.ke (Viona Ojiambo), mathewkiny@jkuat.ac.ke (Mathew Kinyanjui), memkimathi@gmail.com (Mark Kimathi).

most common because it is dependent on the flow velocity and void fraction. Mazumder and Siddique [4] performed Computational fluid dynamics (CFD) analysis for a two-phase air-water flow through a horizontal to vertical 90^0 elbow with a 12.7 mm pipe diameter. A mixture model was used to account for different gas and liquid velocities to solve continuity, momentum and energy equations. CFD analysis results showed a decrease in pressure as fluid leaves the elbow in addition to a larger pressure drop at higher air velocities.

Two-phase flow may occur in convergent pipes such as a venturi that conserves momentum leading to formation of Jeffrey-Hamel flows which is a subject that has been explored by many researchers.[5]Umar et al. studied flow of a viscous incompressible fluid in a converging-diverging channel. The non-linear partial differential equations were transformed to ordinary differential equations by use of similarity transforms. The method of Variation of Parameters (VPM) was then used to solve the Ordinary Differential Equations. It was established that VPM method is more efficient since it requires less computational time but still maintains high accuracy levels. [6] Gerdroodbary et al. studied the influence of thermal radiation on the Jeffrey-Hamel flows. Similarity transformations was used to transform the non-linear partial differential equations to ordinary differential equations. The transformed equations were then solved analytically by applying integral methods. Local skin friction and heat transfer was discussed. It was established that temperature profiles increase with increase in thermal radiation parameters. [7] Umar et al. studied Jeffrey-Hamel flow of a non-Newtonian fluid called a casson fluid. Similarity transforms was applied to reduce the non-linear partial differential equations to Ordinary differential equations. The VPM method and Runge Kutta method of order 4 were then used to solve the resultant equations. Both methods gave out similar results.[19]Alam et al. studied an unsteady two-dimensional laminar forced convective hydrodynamic heat and mass transfer flow of nanofluid along a permeable stretching/shrinking wedge with second order slip velocity using BuongiornoâĂŹs mathematical model. The flow consideration was Jeffrey-Hamel. Using appropriate similarity transformations, the governing non-linear partial differential equations are reduced to a set of non-linear ordinary differential equations which are then solved numerically using the function bvp4c from MATLAB for different values of the parameters. Numerical results for the nondimensional velocity, temperature and nanoparticle volume fraction profiles as well as local skin-friction coefficient, local Nusselt number and local Sherwood number for different material parameters such as wedge angle parameter, unsteadiness parameter, Lewis number, suction parameter, Brownian motion parameter, thermophoresis parameter, slip parameter and Biot number were displayed in graphically as well as tabular form and discussed them from the physical point of view. The obtained numerical results clearly indicate that the flow field is influenced significantly by the second order slip parameter as well as surface convection parameter.

[8] Nizami and Sutopo modelled silica scaling deposition in geothermal wells. He was able to come up with a model that predicts silica scaling growth in the two-phase geothermal pipes. Temperature profiles were the most important variable that he considered in his model formulation.

Studies on thermophoresis have also been of great contribution to research.[9]Bosworth et al. measured the negative force of thermophoretic force on a macroscopic spherical particle. Size scaling was done by matching Knudsen numbers to microscale particles such as aerosol droplets at atmospheric pressure. [10] Rahman et al. studied , the influence of magnetic field and thermophoresis on unsteady two-dimensional forced convective heat and mass transfer flow of a viscous, incompressible and electrically conducting fluid along a porous wedge in the presence of the temperature-dependent thermal conductivity and variable Prandtl number have been studied numerically. He established that the thermophoretic particle deposition velocity significantly influenced by the magnetic field parameter. Moreover, it was found that the rate of heat transfer significantly influenced by the variation of the thermal conductivity and Prandtl number.[18] Mkwizu et al. investigated the combined effects of thermophoresis, Brownian motion and variable viscosity on entropy generation in a transient generalized Couette flow of nanofluids with Navier slip and convective cooling of water-based nanofluids containing Copper and Alumina as nanoparticles. Both first and second laws of thermodynamics are applied to analyse the problem. The nonlinear governing equations of continuity, momentum, energy and nanoparticles concentration were tackled numerically using a semi discretization finite difference method together with Runge-Kutta Fehlberg integration scheme. Numerical results for velocity, temperature, and nanoparticles concentration profiles were obtained and utilised to compute the entropy generation rate, irreversibility ratio and Bejan number. Pertinent results were displayed graphically and discussed quantitatively. It was established that careful combination of parameter values, the entropy production within the channel flow in a variable viscosity transient generalized Couette flow of nanofluids with Navier slip and convective cooling water based nanofluids can be minimised.

Previous studies on Jeffrey-Hamel flows have not considered the problem of silica deposition in modeling geothermal flows as a result of thermophoresis effect. This phenomena should be emphasized for a model to adequately describe fluid flows in geothermal plants. This study shall model the Jeffrey-Hamel flow of a geothermal fluid with non-linear viscosity and skin friction based on the previous study of [11] Nagler inside a convergent wedge. The concentration equation shall be introduced to govern the concentration of silica particles. The body forces shall comprise of forces due to concentration of silica deposits and temperature gradient. The fluid flow shall be two-phase with silica particles depositing radially on the sides of the pipe. The non-linear viscosity which is as a result of changes in temperature and concentration gradients shall be a function of T and θ in the liquid phase. Whereas in the gaseous phase the variable viscosity shall be a function of θ only.

2.   Mathematical Model

We consider two-phase flow in a geothermal pipe with convergent wedges (non-parallel walls) as shown in the Fig. 1 below. The fluid is incompressible, two-dimensional and of non-linear viscosity. Further, the fluid flow is unsteady
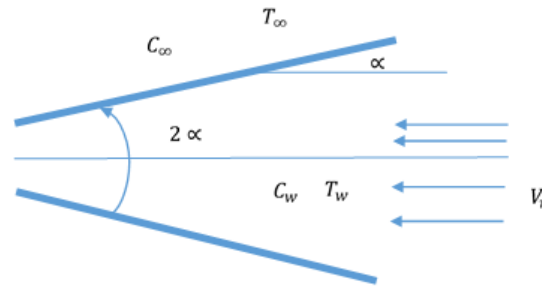

Fig. 1. Flow configuration

with radial motion that is dependent on r,θ and t. The power law model has been used to govern the non-newtonian behavior of both phases. Viscosity is a non-linear function of T and θ in the liquid phase and a function of θ only in the gaseous state. There exists an annulus flow regime with the gaseous phase centrally placed while the liquid phase is on the walls.A slip interphase separates the two phases. Bouyancy forces drive the fluid, viscous dissipation provides the source of energy while thermophoresis enables movement of the silica particles in both phases. There is a correction factor that accounts for silica scaling deposition. The governing equations are equation of mass, momentum, energy and concentration.

$$\frac{\rho}{r}\frac{\partial}{\partial r}(rV_r) = 0 \tag{1}$$

$$\hat{r}: \rho\left(\frac{\partial V_r}{\partial t} + V_r\frac{\partial V_r}{\partial r}\right) = -\frac{\partial P}{\partial r} + \frac{1}{r}\tau_{rr} + \frac{\partial}{\partial r}(\tau_{rr}) + \frac{1}{r}\frac{\partial}{\partial \theta}(\tau_{\theta r}) - \frac{\tau_{\theta\theta}}{r} + g_r\beta(T - T_\infty) + g_r\beta^\star(C - C_w) \tag{2}$$

$$\hat{\theta}: 0 = -\frac{1}{\rho r}\frac{\partial P}{\partial \theta} + \left(\frac{1}{\rho r^2}\frac{\partial}{\partial r}(r^2\tau_{r\theta}) + \frac{1}{\rho r}\frac{\partial}{\partial \theta}(\tau_{\theta\theta}) + \frac{\tau_{\theta r} - \tau_{r\theta}}{\rho r}\right) + \frac{g_\theta\beta}{\rho}(T - T_\infty) + \frac{g_\theta\beta^\star}{\rho}(C - C_w) \tag{3}$$

$$\rho C_p\left(\frac{\partial T}{\partial t} + V_r\frac{\partial T}{\partial r}\right) = k_f\left(\frac{1}{r}\frac{\partial}{\partial r}\left(r\frac{\partial T}{\partial r}\right) + \frac{1}{r^2}\frac{\partial^2 T}{\partial \theta^2}\right) + \mu\left(2\left(\frac{\partial V_r}{\partial r}\right)^2 + 2\left(\frac{V_r}{r}\right)^2 + \left(\frac{1}{r}\frac{\partial V_r}{\partial \theta}\right)^2\right) \tag{4}$$

$$\frac{\partial C}{\partial t} + V_r\frac{\partial C}{\partial r} = D\left(\frac{1}{r}\frac{\partial}{\partial r}\left(r\frac{\partial C}{\partial r}\right) + \frac{1}{r^2}\frac{\partial^2 C}{\partial \theta^2}\right) + \frac{1}{r}\frac{\partial}{\partial \theta}(V_{T\theta}C) - \psi C \tag{5}$$

The thermophoretic velocty V_T, was recommended by [13]Talbot et al. and is expressed as:

$$V_T = \frac{-k\nu}{T}\nabla T \tag{6}$$

where $k\nu$ represents the thermophoretic diffusivity and k is the thermophoretic coefficient which ranges in value from 0.2 to 1.2 as indicated by [12] Batchelor and Shen. The power law model has been used to define viscosity as follows:

$$\mu = \mu_0 g^{n-1}, g = g(\theta) \tag{7}$$

The piecewise definition for viscosity for both the gaseous and the liquid phase are as follows:

$$g = \begin{cases} \theta^s & for\, s \neq 0 \quad (gaseous\ phase) \\ \frac{\theta^s}{1+\gamma(T-T_\infty)} & or\, s\, and\, \gamma \neq 0 \quad (liquid\ phase) \end{cases} \tag{8}$$

where s and γ are constants and θ is the wedge angle.

θ is a subset of angle α. For the total angle 2α of the wedge, $2\alpha\|omega\pi$. The wedge angle parameter is given by Rahman et al. [10] as

$$\Omega = \frac{m}{m+1} \tag{9}$$

For a convergent Jeffrey-Hamel flow to occur the value of Ω must not exceed 180° or π radians. If it exceeds the flow becomes a couette flow

3. Boundary Conditions

The boundary conditions for the above stated model are as follows: For the gaseous phase we have $\theta \epsilon \left(0, \frac{3}{5}\alpha\right)$

$$V_r = 1 \quad \frac{\partial V_r}{\partial \theta} = 0 \quad T = T_w \quad C = C_w \qquad as \quad \theta = 0$$

$$V_r = 0.3 \qquad T = 0.7 T_w \quad C = 0.7 \quad C_\infty \quad as \, \theta = \pm \frac{3}{5}\alpha \tag{10}$$

For the liquid phase we have:
$\theta \epsilon \left(\frac{3}{5}\alpha, \alpha\right)$

$$V_r = 0.3 \quad \frac{\partial V_r}{\partial \theta} = 0 \quad T = 0.7 T_w \quad C = 0.7 C_\infty \quad as \quad \theta = \pm \frac{3}{5}\alpha$$

$$V_r = 0 \qquad T = T_\infty \quad C = C_\infty \quad as \quad \theta = \pm \alpha \tag{11}$$

where

$$V_r (\theta, t) = -\frac{Q}{r} \frac{1}{\delta^{m+1}} f(\eta) \tag{12}$$

see [17] Sattar et al. and [11]Naglar et al. m is a parameter that is related to the wedge angle while δ is defined as the time-dependent length scale[more details in [14]Sattar,[15] Alam and Huda and [16] Alam et al.].

$$\delta = \delta(t) \tag{13}$$

Q is the planar volumetric flow rate as defined by [11]Naglar et al.

4. Nondimensionalization

Nondimensionalization is the process of converting dimensional quantities to non-dimensional quantities. This technique is used to simplify and parameterize problems where measured units are involved.In this study the following nondimensional variables shall be applied to simplify the problem:

$$\frac{\omega(\eta)}{\delta^{m+1}} = \frac{T - T_\infty}{T_w - T_\infty} \tag{14}$$

$$\frac{\phi(\eta)}{\delta^{m+1}} = \frac{C - C_w}{C_\infty - C_w} \tag{15}$$

where η is the similarity variable. Employing Eqs. (13),(15) and (16) into Eqs. (1) to (5) we have: For gaseous phase we have:

$$-\left((n-1)\left(s(s-1)\theta^{sn-s-2} + s^2(n-2)\theta^{sn-s-2}\right)\right) f' - s(n-1)\theta^{sn-s-1}\left(2f'' + 4f\right)$$

$$-\theta^{sn-s}\left(4f' + f'''\right) + \frac{2Re}{\delta^{m+1}} f'f - (m+1)\frac{r^{m+1}}{\delta^{m+1}}\lambda f' + \frac{g_r G_{r(T)}}{Q}\left(\omega' - \omega\right) + \frac{g_r G_{r(C)}}{Q}\left(\phi' - \phi\right) = 0 \tag{16}$$

$$\frac{1}{Pr}\omega'' + \frac{r^{m+1}}{\delta^{m+1}}(m+1)\lambda\omega + \frac{Ec\theta^{sn-s}}{r^2\delta^{(m+1)}}\left(4f^2 + \left(f'\right)^2\right) = 0 \tag{17}$$

$$\frac{1}{S_c}\phi'' + (m+1)\frac{r^{m+1}}{\delta^{m+1}}\lambda\phi - \frac{k\theta^{sn-s}}{\left(\omega + N_t\delta^{(m+1)}\right)}\left(\phi'\omega' - \frac{\phi + N_c\delta^{(m+1)}}{\omega + N_t\delta^{(m+1)}}\left(\omega'\right)^2 + \left(\phi + N_c\delta^{(m+1)}\right)\omega'\right)$$

$$-\frac{ks(n-1)\theta^{sn-s-1}}{\delta^{(m+1)}}\left(\frac{\phi + N_c\delta^{(m+1)}}{\omega + N_t\delta^{(m+1)}}\right)\omega' - \frac{\psi}{\delta^{m+1}}\left(\phi + N_c\delta^{(m+1)}\right) = 0 \tag{18}$$

For the liquid phase we have:

$$-(n-1)\left(\frac{\theta^s \delta^{m+1}}{\delta^{m+1}+d\omega}\right)^{n-2}\left(s(s-1)\theta^{s-2}-\frac{d\theta^s \omega'+2sd\theta^{s-1}\omega'}{(\delta^{m+1}+d\omega)}-\frac{2\theta^s d^2(\omega')^2}{(\delta^{m+1}+d\omega)^2}\right)f'$$

$$-(n-1)(n-2)\theta^{sn-3s}\left(\frac{\delta^{m+1}}{\delta^{m+1}+d\omega}\right)^{n-2}\left(s\theta^{s-1}-\frac{\theta^s d\omega'}{(\delta^{m+1}+d\omega)}\right)^2 f'$$

$$-(n-1)\theta^{sn-2s}\left(\frac{\delta^{m+1}}{\delta^{m+1}+d\omega}\right)^{n-1}\left(s\theta^{s-1}-\frac{\theta^s d\omega'}{(\delta^{m+1}+d\omega)}\right)(2f''+4f)$$

$$-\left(\frac{\theta^s \delta^{m+1}}{\delta^{m+1}+d\omega}\right)^{n-1}(4f'+f''')+\frac{2Re}{\delta^{m+1}}f'f-(m+1)\frac{r^{m+1}}{\delta^{m+1}}\lambda f'$$

$$+\frac{g_r G_{r(T)}}{Q}(\omega'-\omega)+\frac{g_r G_{r(C)}}{Q}(\phi'-\phi)=0 \tag{19}$$

$$\frac{1}{Pr}\omega''+\frac{r^{m+1}}{\delta^{m+1}}(m+1)\lambda\omega+\frac{Ec\theta^{sn-s}\delta^{(m+1)(n-2)}}{r^2(\delta^{m+1}+d\omega)^{n-1}}\left(4f^2+(f')^2\right)=0 \tag{20}$$

$$\frac{1}{S_c}\phi''+(m+1)\frac{r^{m+1}}{\delta^{m+1}}\lambda\phi$$

$$-\frac{k}{(\omega+N_t\delta^{(m+1)})}\left(\frac{\theta^s \delta^{m+1}}{\delta^{m+1}+d\omega}\right)^{n-1}\left(\phi'\omega'-\frac{\phi+N_c\delta^{(m+1)}}{\omega+N_t\delta^{(m+1)}}(\omega')^2+(\phi+N_c\delta^{(m+1)})\omega'\right)$$

$$-\frac{k(n-1)\theta^{sn-2s}}{\delta^{(m+1)}}\left(\frac{\delta^{m+1}}{\delta^{m+1}+d\omega}\right)^{n-1}\left(s\theta^{s-1}-\frac{\theta^s d\omega'}{(\delta^{m+1}+d\omega)}\right)\left(\frac{\phi+N_c\delta^{(m+1)}}{\omega+N_t\delta^{(m+1)}}\right)\omega'$$

$$-\frac{\psi}{\delta^{m+1}}\left(\phi+N_c\delta^{(m+1)}\right)=0 \tag{21}$$

The non-dimensionalized boundary conditions are therefore given by:
For the gaseous phase we have:
$\theta\epsilon\left(0,\frac{3}{5}\alpha\right)$

$$f(0)=1 \quad f'(0)=0 \quad \omega(0)=\delta^{m+1} \quad \phi(0)=0 \quad as \quad \eta=0$$

$$f\left(\frac{3}{5}\alpha\right)=0.3 \quad \omega\left(\frac{3}{5}\alpha\right)=0.7\delta^{m+1} \quad \phi\left(\frac{3}{5}\alpha\right)=0.7\delta^{m+1} \quad as \quad \eta=\pm\frac{3}{5}\alpha \tag{22}$$

For the liquid phase we have
$\theta\epsilon\left(\frac{3}{5}\alpha,\alpha\right)$

$$f\left(\frac{3}{5}\alpha\right)=0.3 \quad f'\left(\frac{3}{5}\alpha\right)=0 \quad \omega\left(\frac{3}{5}\alpha\right)=0.7\delta^{m+1} \quad \phi\left(\frac{3}{5}\alpha\right)=0.7\delta^{m+1} \quad as \quad \eta=\pm\frac{3}{5}\alpha$$

$$f(\alpha)=0 \quad \omega(\alpha)=0 \quad \phi(\alpha)=\delta^{m+1} \quad as \quad \eta=\pm\alpha \tag{23}$$

The non-dimensional numbers obtained from the above equations are: $Re=\frac{Q\rho}{\mu_0}$ is the Reynolds' number, $G_{r(T)}=\frac{\beta r^3(T_w-T_\infty)}{\mu_0}$ is the Grasshoff number due to temperature, $G_{r(C)}=\frac{\beta^\star r^3(C_\infty-C_w)}{\mu_0}$ is the mass Grasshoff number, $Pr=\frac{\mu_0 C_p}{k_f}$ is the Prandtl number, $Ec=\frac{Q^2}{C_p(T_w-T_\infty)}$ is the Eckert number, $Sc=\frac{\mu_0}{D}$ is the Schmidt number, $Nt=\frac{T_\infty}{(T_w-T_\infty)}$ is the thermophoresis parameter and $Nc=\frac{C_w}{(C_\infty-C_w)}$ is the concentration ratio. The unsteadiness parameter is defined by

$$\lambda=\frac{\delta^m}{vr^{m-1}}\frac{d\delta}{dt} \tag{24}$$

where

$$v = \frac{\mu}{\rho} \tag{25}$$

δ is the the time-dependent length scale, m is a parameter related to the wedge angle and r is the radius of the pipe. Suppose that

$$\lambda = \frac{c}{r^{m-1}} \tag{26}$$

where c is a constant such that

$$c = \frac{\delta^m}{v} \frac{d\delta}{dt} \tag{27}$$

Integrating by separation of variables yields:

$$\delta = [c(m+1)vt]^{\frac{1}{m+1}} \tag{28}$$

Taking c=2 and m=1 we obtain

$$\delta = 2\sqrt{vt} \tag{29}$$

$\delta(t)$ is called a time-dependent length scale because its dimensions are L.

5.   Numerical Technique

The Bvp4c is MATLAB solver based on collocation method that provides continuous solution with a 4th order accuracy in the interval of integration. The method uses a mesh of points to divide the interval of integration into sub-intervals. Each sub-interval is solved based on the system of algebraic equations and the boundary equations provided. The solver then estimates the error of the numerical solution on each sub interval. If the solution does not satisfy the tolerance criteria, the solver adapts the mesh and repeats the process.The user must provide the points of the initial mesh as well as an initial approximation of the solution at the mesh points. This method was used to solve the above stated governing equations because of the following advantages:

1. The method is not expensive since it reduces the computation time.

2. The method is able to give optimal solutions that are accurate.

3. The method is convergent because when you reduce or increase the step size the solution still tends to the exact solution.

6.   Results and Discussions
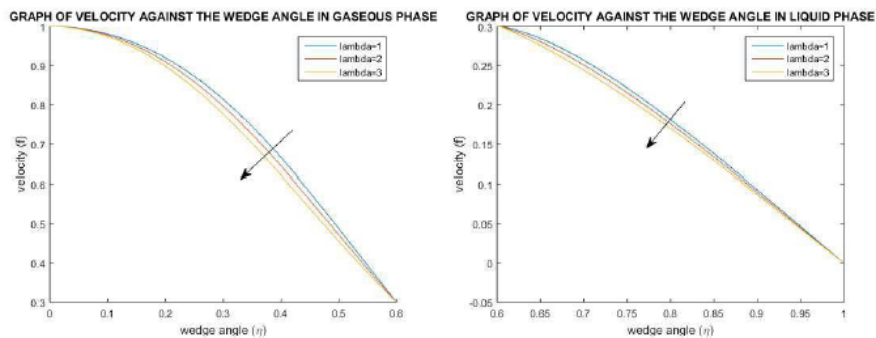
Fig. 2. Graph of Velocity against Wedge angle for $\lambda = 1.0, 2.0, 3.0$

From Fig. 2 it is observed that as the unsteadiness parameter λ increases, the velocity in both the gaseous and liquid phase decreases. By definition in Eqs. (12) and (24), the unsteadiness parameter λ and the time dependent length scale δ have a direct relationship. Consequently resulting to decrease in the velocity V_r which has an inverse relationship with the time dependent length scale δ. From Fig. 3 it is observed that as the unsteadiness parameter λ increases,
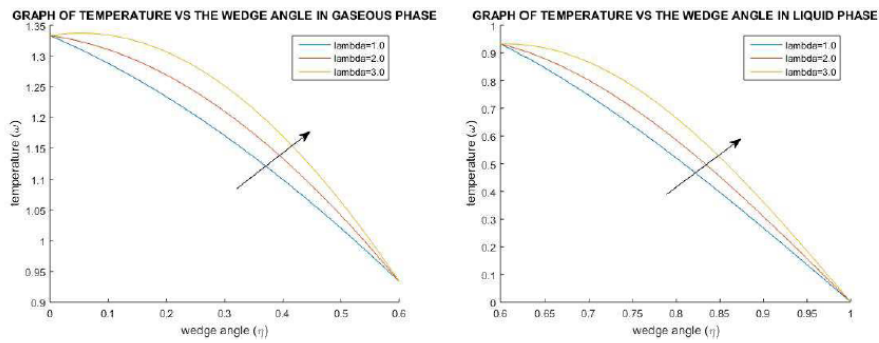
Fig. 3. Graph of Temperature against Wedge angle for $\lambda = 1.0, 2.0, 3.0$
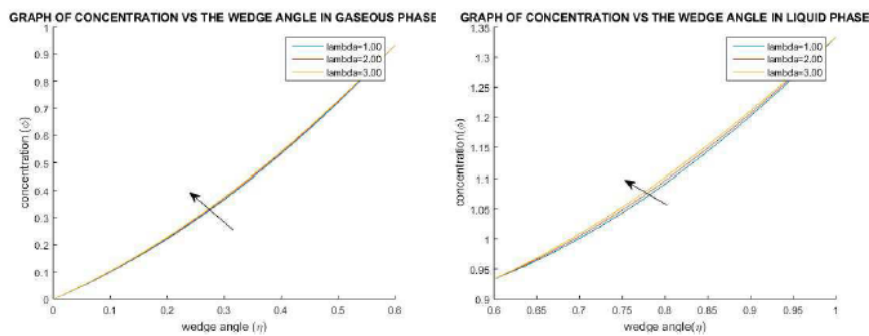

Fig. 4. Graph of Concentration against Wedge angle for $\lambda = 1.0, 2.0, 3.0$

the temperature in both the gaseous and liquid phase decreases. From Newton's law of cooling the rate of heat loss of a body $\frac{\partial T}{\partial t}$, is directly proportional to the difference in the temperatures between the body and its surrounding $T - T_\infty$, provided that the temperature difference is small and the nature of the radiating surface remains the same. From Eqs. (14) (24) above an increase in the unsteadiness parameter λ implies an increase in time dependent length scale. This leads to an increase in the rate of heat loss $\frac{\partial T}{\partial t}$, which is directly related to $T - T_\infty$. This consequently results to an increase in temperature as shown in Fig. 3. From Fig. 4 it can be observed that as the unsteadiness parameter λ increases, the concentration in both the gaseous and the liquid phase decreases. Decrease in temperature of the fluid leads to increase in the concentration of colloidal silica particles. Increase in unsteadiness parameter leads to increase in temperature profiles as shown in Fig. 3. As the temperature increases the silica particles become soluble thereby decreasing in concentration. From Fig. 5 the velocity increase is more pronounced in the gaseous phase in comparison
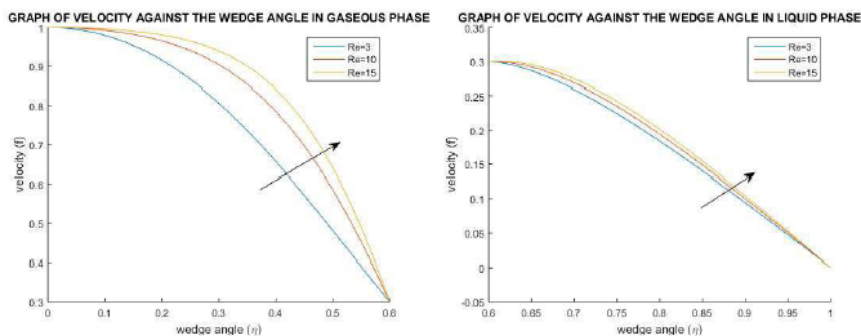

Fig. 5. Graph of Velocity against Wedge angle for $Re = 3.0, 10.0, 15.0$

to the liquid phase. This is as a result of; Firstly, an increase in the Reynold's number Re implies an increase in the fluid velocity due to the direct relationship they have by definition. Secondly, the gaseous phase is less viscous in comparison to the liquid phase because viscosity is a non-linear function of θ only in the gaseous phase while it is a function of both θ and T in the liquid phase. The lower the viscous forces the higher the Reynolds number leading to pronounced

increase in the gas velocity in comparison to the liquid velocity. As shown in Fig. 6, an increase in the value of Grasshof
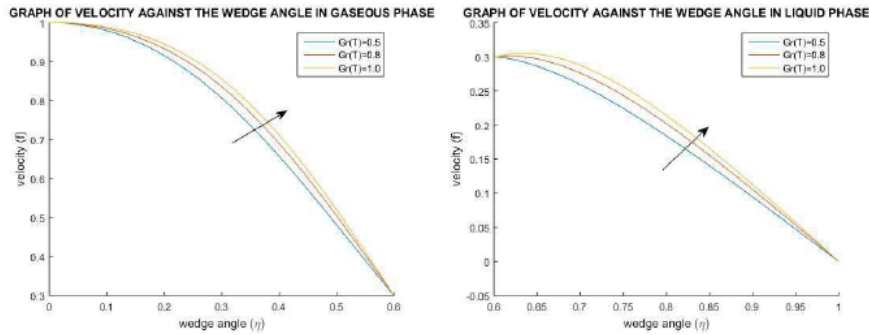

Fig. 6. Graph of Velocity against Wedge angle for $Gr\,T = 0.5, 0.8, 1.0$

number or any buoyancy related parameter implies an increase in the temperature difference $T_w - T_\infty$ and this makes the bond(s) between the fluid to become weaker, strength of the internal friction to decrease. This results to increased movement of the fluid particles thus resulting to increased fluid velocity in both phases. Increased buoyancy forces results to increased applied forces which accelerates the motion of the fluid particles resulting to increased velocity of the fluid.
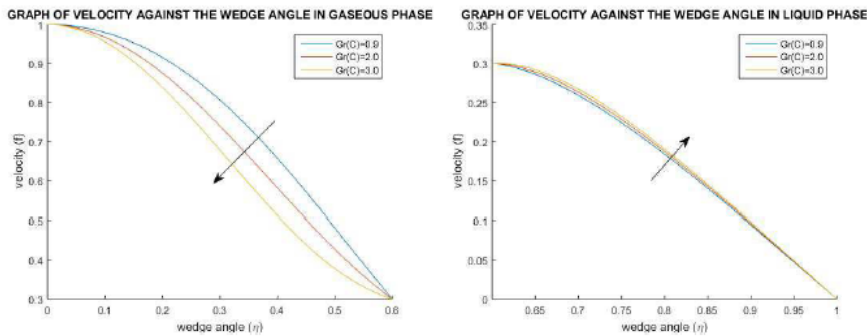

Fig. 7. Graph of Velocity against Wedge angle for $GrC = 0.9, 2.0, 3.0$

From Fig. 7, an increase in the value of mass Grasshof number number implies an increase in the concentration difference i.e. $(C_\infty - C_w)$. This means that the concentration of silica particles at the wall C_∞ is increasing compared to that in the free stream. This results to decrease in the concentration of silica particles in the gaseous phase but increase in the concentration of the silica particles in the liquid phase. From Fig. 8 the temperature variation with
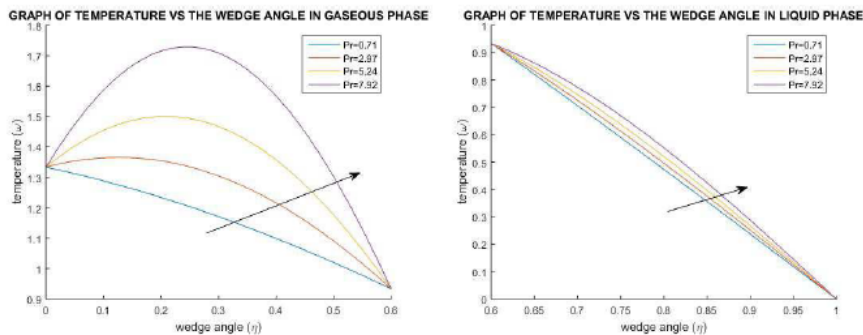

Fig. 8. Graph of Temperature against wedge angle for $Pr = 0.71, 2.97, 5.24, 7.92$

increased Pr in the gaseous phase is more pronounced in comparison to the liquid phase this is due to increased heat capacity allows for retention of temperature thereby increasing the temperature values. In Fig. 9 it is observed that an increase in the Eckert number when λ and Pr are held constant leads to an increase in temperature. An increase in the Eckert number implies a decrease in the temperature difference $T_w - T_\infty$. This shows that the free stream temperature
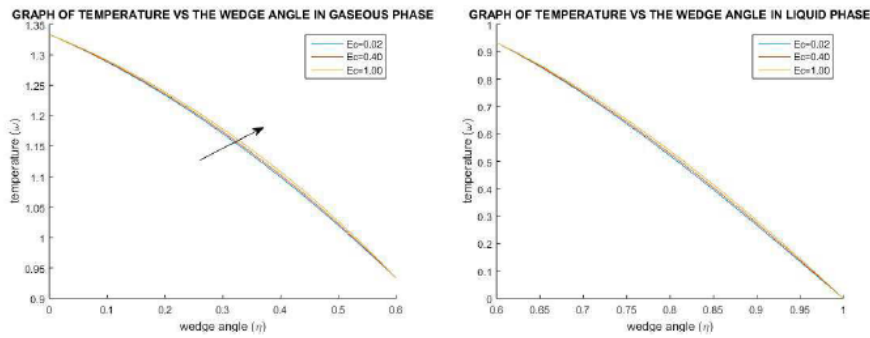
Fig. 9. Graph of Temperature against wedge angle for $Ec = 0.02, 0.40, 1.00$

is decreasing in comparison to the wall temperature which is increasing. This implies increase in temperature with increase in the wedge angle. In Fig. 10 increase in the Schmidt number Sc leads to decrease in the mass diffusivity D
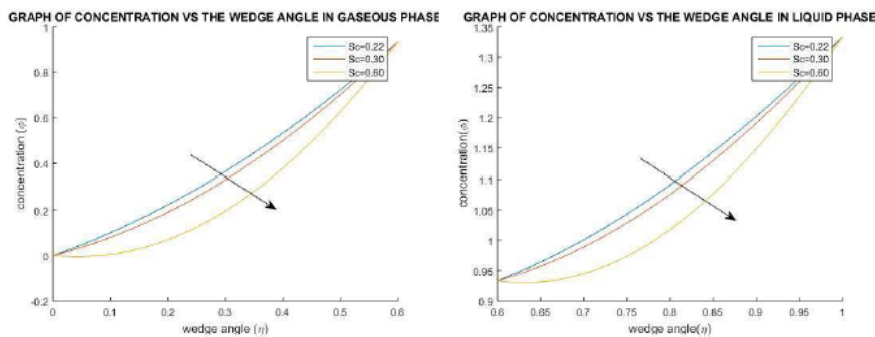

Fig. 10. Graph of Temperature against wedge angle for $Sc = 0.22, 0.30, 0.60$

due to their inverse relationship. Decrease in mass diffusivity implies decreased movement of colloidal silica particles which decreases the concentration of silica particles. Increase in the concentration ratio Nc implies decrease in the
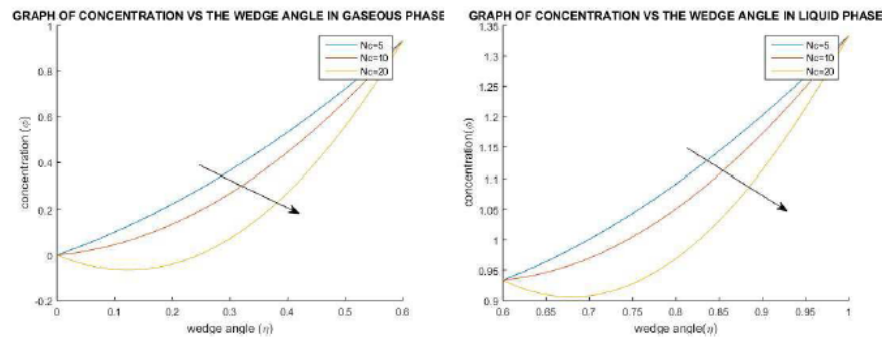

Fig. 11. Graph of Temperature against wedge angle for $Nc = 5.0, 10.0, 20.0$

concentration difference $C_\infty - C_\omega$. This means that the concentration of silica particles at the walls is decreasing but increasing at the radial axis. This implies that the particles are moving centrally; thereby decreasing with increase in the wedge angle in both phases as shown in Fig. 11. From Fig. 12, Increase in the thermophoresis parameter Nt implies decrease in the temperature difference$(T_w - T_\infty)$. This means that the wall temperature T_∞ is increasing resulting to movement of the silica particles towards the radial axis. In Fig. 13 it is observed that an increase in ψ when Sc , Nt , Nc and λ are held constant leads to a decrease in the concentration of silica particles. ψ represents the correction factor for silica concentration. The methods of preventing silica deposition are given different rank values which can be represented by ψ . The first and the most used rank is flashing the geothermal fluid to pressures below the saturation index, the second rank is to adjust the levels of PH so as to keep silica in solution and therefore present
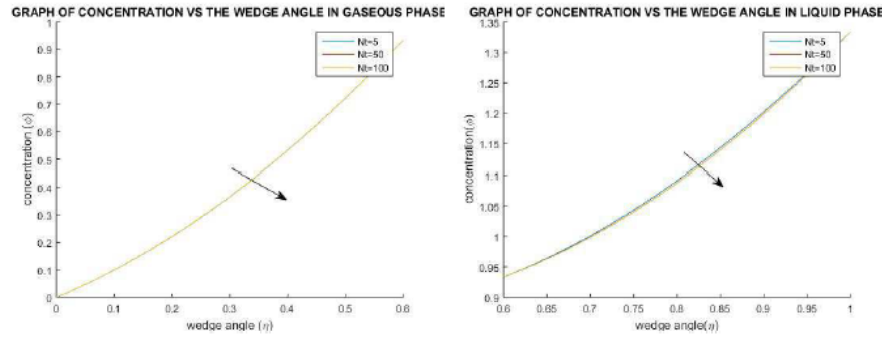
Fig. 12. Graph of Concentration against wedge angle for $Nt = 5.0, 50.0, 100.0$
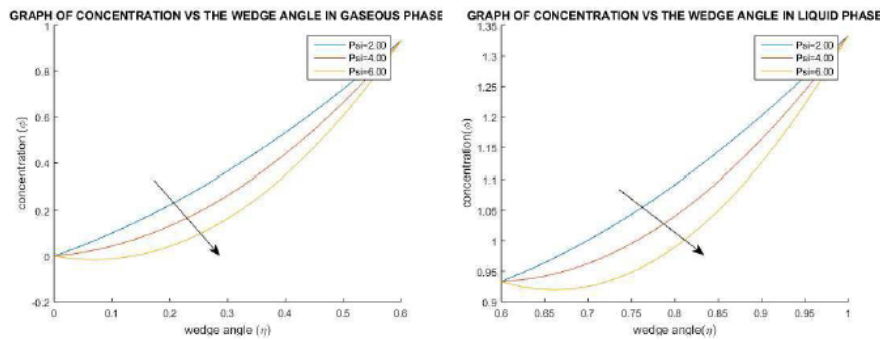

Fig. 13. Graph of Concentration against wedge angle for $\Psi = 2.0, 4.0, 6.0$

deposition, the third rank is adding condensate to brine to dilute it and prevent super-saturation, the fourth rank is to apply commercially available inhibitors.

7. Validation

Comparison of results with Naglar [11] article proved to be in good agreement. It is found that the velocity decreases gradually with the tangential direction progress and Increase in the Reynolds number Re causes the velocity function values to increase. Further the nonlinear viscosity term has influential effects on the flow. These results are observed in both the liquid and the gaseous phase.

8. Conclusion

A two-phase flow in a geothermal pipe with convergent wedges (non-parallel walls) has been modeled with four governing equations; equation of mass, equation of momentum, equation of energy and equation of concentration.It is established that the unsteadiness parameter significantly influences the velocity, temperature and concentration in both the gaseous and the liquid phase, secondly the Reynolds'number effect in the gaseous phase velocity is more significant incomparison to the liquid phase, thirdly the variation in heat transfer as a result of the Prandtl number is more significant in comparison to the liquid phase, fourthly there is a significant effect of the control factor introduced in the concentration equation to counter silica polymerization . Thus in a geothermal pipe, the gaseous and the liquid phase have to be accounted separately as a result of these these variations. Further, the control mechanisms used for preventing silica deposition need to be factored in the concentration equations with their ranking specification so as to monitor the growth of silica deposits.

In summary the following conclusions are made:

1. The unsteadiness parameter has an effect on the velocity, temperature and concentration profiles. Increase in the unsteadiness parameter λ ,leads to decrease in the flow velocity in both the liquid and the gaseous phase. However, increase in λ leads to decrease in the temperature and concentration levels in both the liquid and the gaseous phase.

2. The Reynold's number *Re* influences the flow velocity in both the liquid and the gaseous phase. However, its effect are more pronounced in the gaseous phase due to low viscosity that allows for diffusion of the gaseous fluid molecules. In the liquid phase viscosity varies inversely with temperature, therefore decrease in temperature leads to increased viscosity which implies increased adhesive forces that impacts on the fluid velocity.

3. An increase in any buoyancy related parameter i.e. $Gr_{(T)}$ and $Gr_{(C)}$ implies an increase in the wall temperature. This results to weakening if the bonds that hold the fluid molecules in both the liquid and the gaseous phase thereby decreasing the fluid velocity.

4. An increase in the Prandtl number *Pr* leads to increased heat capacity when thermal conductivity is a constant. Consequently, this allows for increased temperature.

5. An increase in the Eckert number *Ec* leads to increased radial temperature which results to increased temperature gradient.

6. An increase in the Schmidt number *Sc* leads to decreased mass diffusivity leading to decreased concentration of the silica particles.

7. In order to control the rate of heat transfer and mass transfer in the geothermal pipe the walls of the geothermal pipe should tend to no inclination. There is a lot of deposition and loss of heat that is found in convergent geothermal pipes.

8. The methods of preventing silica deposition are given different rank values which can be represented by ψ

9. The first and the most used rank is flashing the geothermal fluid to pressures below the saturation index, the second rank is to adjust the levels of PH so as to keep silica in solution and therefore present deposition, the third rank is adding condensate to brine to dilute it and prevent super-saturation, the fourth rank is to apply commercially available inhibitors.

Acknowledgements

References

[1] J. Polii and H. Abdurrachim,Model Development of Silica Scaling Prediction on Brine Flow Pipe, Proceedings, 13th Indonesia International Geothermal Convention and Exhibition, Jakarta, Indonesia, (2013) 12 âĂŞ 14.

[2] A. Hasan and C. Kabir, Modelling two-phase fluid and heat flows in geothermal wells, J. of Petroleum Science and Engineering 71(2003),(2010) 77-86.

[3] H. Palsson, E. Berghorsson and O. Palsson, Estimation and validation of models two phase flow geothermal wells, Proceedings of 10th international symposium of heating and cooling, (2006)

[4] H. Mazumder and A. Siddique, CFD analysis of two-phase flow characteristic in a 90 degree elbow, J. of mechanical engineering. University of Michigan. 3(3) (2011).

[5] K. Umar, A. Naveed, Z. Zaidi , S. Jan and T. Syed, On Jeffrey-Hamel flows, Int. J. of Modern Mathematical Sciences. 7(3)(2013) 236-267.

[6] Gerdroodbary, M. Barzegar, M. Rahimi. and D. Ganji, Investigation of thermal radiation Jeffrey Hamel flow to stretchable convergent/ divergent channels. Science direct, Elsevier case studies in thermal engineering. 6 (2015) 28-39.

[7] K. Umar, A. Naveed, S. Waseen , T. Syed and D. Mohyud, Jeffrey-Hamel flow for a non-Newtonian fluid, J. of Applied and Computational Mechanics. 2(1) (2016) 21-28.

[8] K. Nizami and Sutopo, Mathematical modeling of silica deposition in geothermal wells, 5th International Geothermal Workshop (IIGW2016), IOP Conference series: Earth and Environmental Science (2016)2016

[9] R. Bosworth, A. Ventura, A. Ketsdever and S. Gimelchein, Measurement of negative thermophoretic force, Journal of Fluid Mechanics. 805(2016) 207-221.

[10] A. Rahman, M. Alam and M. Uddin, Influence of magnetic field and thermophoresis on transient forced convective heat and mass transfer flow along a porous wedge with variable thermal conductive and variable thermal conductivity and variable Prandtl number, Int. J. of Advances in Applied Mathematics and Mechanics. 3(4) (2016) 49-64.

[11] J. Nagler J., Jeffrey-Hamel flow on non-Newtonian fluid with nonlinear viscosity and wall friction, J. of Applied Mathematics and Mechanics. 38(6)(2017) 815-830.

[12] G. Batchelor and C. Shen, Thermophoretic deposition of particles in gas flowing over cold surface, J. of colloid interphace science, 107 (1985) 21-37.

[13] L.Talbot, R.Cheng , A. Schefer, D. Wills, Thermophoresis of particles in a heated boundary layer, J. of fluid mechanics. 101 (1980) 737-758.

[14] M. A. Sattar, A local simialrity transformation for the unsteady two-dimensional hydrodynamic boundary layer equations of a flow past a wedge, Int. J. appl.Math. and Mech. 7 (2011) 15-28.

[15] M. S. Alam, M. N. Huda, A new approach for local similarity solutions of an unsteady hydromagnetic free convective heat transfer flow along a permeable flat surface, Int. J. Adv. Appl.Math.Mech. 1(2) (2013) 39-52.

[16] M. S. Alam, M. M. Haque, M. J. Uddin, Unsteady MHD free convective heat transfer flow along a vertical porous flat plate with internal heat generation, Int. J. Adv. Appl.Math.Mech. 2(2) (2014) 52-61.

[17] M. A. Sattar, Derivation of the similarity equation of the 2-D Unsteady Boundary Layer equations and the Corresponding similarity equations, American J. of Fluid Mech. 3(5) (2013) 135-142.

[18] M. H. Mkwizu, A. X. Matofali and N. Ainea, Entropy generation in a variable viscosity transient genralized Coutte flow on nanofluids with Navier Slip and Convective cooling, Int. J. of Adv. in Appied Math. and Mech., 5(4) (2018) 20-29.

[19] M. S. Alam, M. M. Haque and M. J. Uddin, Convective flow of nano fluid along a permeable stretching/shrinking wedge with second order slip using Buongiorno's mathematical model, Int. J. of Adv. in Appied Math. and Mech., 3(3) (2016) 79-91.